Signal Processing 140 (2017) 149–160

Contents lists available at ScienceDirect

Signal Processing

journal homepage: www.elsevier.com/locate/sigpro

Joint DOA estimation and source number detection for arrays with arbitrary geometry

Falamarz Izedi, Mahmood Karimi*, Mostafa Derakhtian

School of Electrical and Computer Engineering, Shiraz University, Shiraz, Iran

ARTICLE INFO

Article history:
Received 22 October 2016
Revised 20 April 2017
Accepted 6 May 2017
Available online 16 May 2017

Keywords:
DOA estimation
Source number detection
Array processing
Nonuniform array

ABSTRACT

In this paper, we focus on the problem of joint direction-of-arrival (DOA) estimation and source number detection for an array of sensors. We propose a CLEAN-based sequential algorithm that uses a sequential hypothesis testing procedure. This method can be employed for any array with an arbitrary geometry. We also manage to reduce the computational complexity of the proposed method. Additionally, we derive an analytical performance bound for the source number detection algorithm. Our simulation results show that the proposed method achieves an appropriate performance even for low SNR or small number of snapshots. It is shown that the proposed method is applicable to both correlated and uncorrelated sources. Unlike popular methods, the algorithm does not require to know the number of sources for the DOA estimation and is able to estimate the number and the DOA of sources jointly.

1. Introduction

Array signal processing has applications in areas such as radar, sonar, wireless communication, radio astronomy, seismology, acoustics, and medical imaging [1,2]. Two of the most important problems in the array signal processing are the direction-of-arrival (DOA) estimation and source number detection. Due to the cost, available space and system performance in practical scenarios, it tends to be unsuitable to restrict the array geometry to a certain class. Therefore, the methods that can be applied to arbitrary array geometries are in great demand [3,4].

For the DOA estimation problem, the multiple signal classification (MUSIC) algorithm [5] is one of the well-known subspace-based methods. This algorithm can be applied to any type of array geometry. A version of this algorithm, which is referred to as root-MUSIC, utilizes polynomial rooting [6]. However, this method is only applicable to the uniform linear array (ULA). In [7] a method is presented to extend the application of the root-MUSIC to the nonuniform linear array case. Fourier-domain root-MUSIC is another method which develops the root-MUSIC algorithm for DOA estimation in the sensor arrays of an arbitrary geometry [8]. Another popular technique for DOA estimation is the estimation of signal parameters via rotational invariance techniques (ESPRIT) [9]. In the ESPRIT method, the array geometry is required to be shift invariant which limits the application of this method to a certain class of arrays. Array interpolation is a DOA estimation technique employed for nonuniform arrays [10–12]. This method involves applying transformation to the received signal in order to obtain an interpolation of the signal over a virtual ULA. Manifold separation technique [13] models the received waveform by means of an orthogonal expansion and approximates the true array steering vector as the product of a matrix that depends only on the array parameters and a Vandermond vector which depends merely on the angle of arrival.

Some other DOA estimation methods are based on a technique called CLEAN [14]. CLEAN is developed initially for radio astronomy. The main idea of CLEAN is to remove the strongest signals from the observed data successively. In [15], a simple version of CLEAN method is applied to the DOA estimation problem. In this simple version, the cancellation of signal components is not perfect and as a result, the performance of DOA estimation degrades. In [3], a method is proposed for DOA estimation in nonuniform linear arrays. This method is a combination of CLEAN, Root-MUSIC and Toeplitz Completion techniques. However, this method needs an initial estimate of DOA of sources and the number of sources must be known.

A popular sequential search technique for finding a sparse solution is orthogonal matching pursuit (OMP) [16]. This method can be utilized for DOA estimation.

Source signals are correlated on condition that multipath reflections are present. When the source signals are correlated, the signal covariance matrix may become rank-deficient and many of the

* Corresponding author.
E-mail addresses: izedi@shirazu.ac.ir (F. Izedi), karimi@shirazu.ac.ir (M. Karimi), derakhtian@shirazu.ac.ir (M. Derakhtian).

http://dx.doi.org/10.1016/j.sigpro.2017.05.008
0165-1684/

mentioned methods fail to find the source DOA [3]. Certain methods such as forward-backward spatial smoothing (FBSS) [18] can be used to improve the rank. The FBSS is one of the best methods to deal with the correlated sources, particularly when ULAs are considered [3]. The disadvantage of this technique is that it uses the subarrays and therefore the resulting covariance matrix size is less than the original covariance matrix size. It must also be pointed out that the FBSS cannot be used directly for an array with an arbitrary geometry.

Regarding the source number detection problem, the minimum description length (MDL) method [19] is one of the most successful methods. Another popular method is Akaike information criterion (AIC) [20]. These methods share common origins in the information-theoretic and Bayesian formulation of the general model selection problem [19]. The MDL and AIC are known to suffer in the detection performance for the small number of snapshots.

In this paper, we propose a CLEAN-based algorithm by solving a sequential generalized likelihood ratio test (GLRT) to estimate both DOA and the number of sources. This method can be used for arrays with an arbitrary geometry. Moreover, we reduce the computational complexity of the proposed method. An analytical performance bound for source number detection is also derived. It has been illustrated that the proposed technique has an appropriate performance in the case of small snapshots for two closely spaced targets. The proposed method is applicable to both correlated and uncorrelated sources. It is noteworthy that the proposed method is a CLEAN-based algorithm that is developed through an statistical approach by solving a sequential generalized likelihood ratio test. It is also worth mentioning that although some versions of CLEAN exist in the literature, there appear to be very few statistical studies about this method [15]. To the best of our knowledge, no other method in the literature looks at the CLEAN algorithm from the GLRT point of view.

The remainder of this paper is organized as follows. Section 2 describes the signal model. The proposed method for the joint DOA estimation and source number detection is presented in Section 3. Section 4 is presented to reduce the computational complexity of the proposed method. The performance bound of the proposed source number detection algorithm, is analyzed in Section 5. Simulation results, presented in Section 6, explore the validation of the theoretical results. Finally, Section 7 concludes the paper.

Notation: Matrices are denoted by the upper boldface letters and vectors by the lower boldface letters. $|x|$ shows the absolute value of x and $\|\mathbf{x}\|$ stands for the Euclidean norm. The superscript ^{H} denotes the Hermitian of a matrix or a vector. $\Pr(\cdot)$ stands for the probability. Furthermore, we use the notation $\mathcal{CN}(\boldsymbol{\mu}, \mathbf{C})$ to indicate the complex normal distribution with the mean $\boldsymbol{\mu}$ and the covariance matrix $\mathbf{C}$. Finally, $\mathbf{I}$ is the identity matrix.

2. The signal model

Consider an array of M omnidirectional sensors with nonuniform spacing in the xy plane. Assume that this array receives signals from $L(L < M)$ narrowband far-field sources with the unknown DOAs, $\boldsymbol{\theta} \triangleq [\theta_1, \ldots, \theta_L]^T$. We intend to estimate the number of sources and their DOAs. The $M \times 1$ array output vector at the nth snapshot can be modeled as [1]:

$$\mathbf{x}(n) = \mathbf{A}_L(\boldsymbol{\theta})\mathbf{s}_L(n) + \mathbf{w}(n), \tag{1}$$

where $\boldsymbol{\theta} = [\theta_1, \ldots, \theta_L]^T$ is the $L \times 1$ vector of signal DOAs. $\mathbf{A}_L(\boldsymbol{\theta}) \triangleq [\mathbf{a}(\theta_1), \ldots, \mathbf{a}(\theta_L)]$ is the $M \times L$ signal steering matrix and $\mathbf{a}(\theta_i)|_{i=1,\ldots,L}$ is the $M \times 1$ steering vector of the ith source which can be expressed as

$$\mathbf{a}(\theta_i) = \Big[\exp\Big(j\frac{2\pi}{\lambda}(x_1 \sin\theta_i + y_1 \cos\theta_i)\Big), \ldots, \times \exp\Big(j\frac{2\pi}{\lambda}(x_M \sin\theta_i + y_M \cos\theta_i)\Big)\Big], \quad i = 1, \ldots, L, \tag{2}$$

where λ is the wavelength of the signal and $\{x_m, y_m\}|_{m=1,\ldots,M}$ are the coordinates of the mth array sensor. $\mathbf{s}_L(n) \triangleq [s_1(n), \ldots, s_L(n)]^T$ is the $L \times 1$ vector of the signal waveforms and $\mathbf{w}(n) \triangleq [w_1(n), \ldots, w_M(n)]^T$ is the $M \times 1$ vector of the complex Gaussian sensor noises with the zero mean and covariance matrix $\sigma^2\mathbf{I}$. Hereafter, for simplicity, we show $\mathbf{A}_L(\boldsymbol{\theta})$ by $\mathbf{A}_L$ and $\mathbf{a}(\theta_i)$ by $\mathbf{a}_i$.

3. The proposed method

In order to estimate the number of sources, we propose a sequential algorithm which results from the solution of a sequential composite hypothesis testing problem. Solving this problem at the ℓth stage will determine whether there is a source in the direction of θ_ℓ or not. The presence or absence of this source must be determined in the presence of the other sources in the unknown direction of $\theta_1, \theta_2, \ldots, \theta_{\ell-1}$. The hypothesis testing problem at the ℓth stage can be modeled as

$$\begin{cases} \mathcal{H}_0^{(\ell)} : \mathbf{x}(n) = \mathbf{A}_{\ell-1}\mathbf{s}_{\ell-1}(n) + \mathbf{w}(n), & n = 1, \ldots, N; \\ \quad \ell = 1, \ldots, L \\ \mathcal{H}_1^{(\ell)} : \mathbf{x}(n) = \mathbf{A}_{\ell-1}\mathbf{s}_{\ell-1}(n) + \mathbf{a}_\ell s_\ell(n) + \mathbf{w}(n), & n = 1, \ldots, N; \\ \quad \ell = 1, \ldots, L, \end{cases} \tag{3}$$

where $\mathbf{A}_{\ell-1}$ is the $M \times (\ell-1)$ steering matrix of $\ell-1$ sources; more explicitly,

$$\mathbf{A}_{\ell-1} \triangleq [\mathbf{a}_1, \ldots, \mathbf{a}_{\ell-1}]. \tag{4}$$

$\mathbf{s}_{\ell-1}(n) \triangleq [s_1(n), \ldots, s_{\ell-1}(n)]^T$ is the $(\ell-1) \times 1$ vector of the signal waveforms and $s_\ell(n)$ is the scalar signal of the ℓth source. This is a composite hypothesis problem with the unknown parameters θ_i and $s_i(n)$ for $i = 1, \ldots, \ell$. The noise variance is assumed to be known. We employ the GLR test to solve the composite hypothesis problem. The details of the derivation of this GLR-based detector is presented in Appendix A. The likelihood ratio is

$$\mathcal{L}_\ell(\mathbf{x}) = \max_\theta \sum_{n=1}^{N} \frac{|\mathbf{a}^H(\theta)\mathbf{P}_{\ell-1}^\perp \mathbf{x}(n)|^2}{\mathbf{a}^H(\theta)\mathbf{P}_{\ell-1}^\perp \mathbf{a}(\theta)} = \sum_{n=1}^{N} \frac{|\mathbf{a}_\ell{}^H \mathbf{P}_{\ell-1}^\perp \mathbf{x}(n)|^2}{\mathbf{a}_\ell{}^H \mathbf{P}_{\ell-1}^\perp \mathbf{a}_\ell} \underset{\mathcal{H}_0^{(\ell)}}{\overset{\mathcal{H}_1^{(\ell)}}{\gtrless}} \eta_\ell, \tag{5}$$

where η_ℓ is the ℓth stage threshold which is determined based on the ℓth stage false alarm probability, $\mathbf{a}_\ell$ is the $M \times 1$ steering vector corresponding to the estimated direction θ_ℓ, and $\mathbf{P}_{\ell-1}^\perp$ is a matrix that is orthogonal to the $\mathbf{A}_{\ell-1}$, and is given by

$$\mathbf{P}_{\ell-1}^\perp = \begin{cases} \mathbf{I} - \mathbf{A}_{\ell-1}\big(\mathbf{A}_{\ell-1}^H \mathbf{A}_{\ell-1}\big)^{-1}\mathbf{A}_{\ell-1}^H & \ell > 1 \\ \mathbf{I} & \ell = 1, \end{cases} \tag{6}$$

and as a result $\mathcal{L}_1(\mathbf{x}) = \sum_{n=1}^{N} \frac{|\mathbf{a}_1{}^H \mathbf{x}(n)|^2}{M}$. Using (5), our CLEAN-based algorithm for joint DOA estimation and source enumeration can be summarized as follows:

Step 1 Compute $\mathcal{L}_1(\mathbf{x})$, and then compare it with the predetermined threshold value, η_1. If this value is not greater than the threshold value, stop the algorithm and $L = 0$. Otherwise $\hat{\theta}_1 = \arg\max_\theta \sum_{n=1}^{N} \frac{|\mathbf{a}^H(\theta)\mathbf{x}(n)|^2}{M}$ and go to the step 2.

Step 2 For $k = 2, 3, \ldots,$ perform the following procedure:

1) Define $\mathbf{A}_{k-1}$ as $\mathbf{A}_{k-1} \triangleq \big[\mathbf{a}_1, \ldots, \mathbf{a}_{k-1}\big]$. Where $\mathbf{a}_{k-1}$ is the steering vector in the direction of $\hat{\theta}_{k-1}$.
2) Compute $\mathbf{P}_{k-1}^\perp$ for $\mathbf{A}_{k-1}$ using (6) and then calculate $\mathcal{L}_k(\mathbf{x})$ from (5).

3) Compare $\mathcal{L}_k(\mathbf{x})$ with the kth stage threshold value.
4) If $\mathcal{L}_k(\mathbf{x})$ is smaller than the threshold, terminate the algorithm. The number of sources is $\hat{L}=k-1$ and the estimated vector of the source directions is $\hat{\boldsymbol{\theta}}=[\hat{\theta}_1,\ldots,\hat{\theta}_{k-1}]^T$.
5) If $\mathcal{L}_k(\mathbf{x})$ is greater than the threshold, solve for $\hat{\theta}_k=\arg\max_\theta \sum_{n=1}^{N}\frac{|\mathbf{a}^H(\theta)\mathbf{P}_{k-1}^{\perp}\mathbf{x}(n)|^2}{\mathbf{a}^H(\theta)\mathbf{P}_{k-1}^{\perp}\mathbf{a}(\theta)}$.
6) Insert $\mathbf{a}_k$ instead of $\mathbf{a}_{k-1}$ into $\mathbf{A}_{k-1}$ then, compute $\mathbf{P}_{k-1}^{\perp}$ and finally calculate (5) to update $\hat{\theta}_{k-1}$.

Please note that the last stage of the step 2 is added to improve the performance of the DOA estimation and source number detection, especially when there are strong sources. In this case, the mentioned stage improves the signal components cancellation and as a result, the residuals will be sufficiently small.

Remark 1. In the case of two-dimensional DOA estimation, the $M\times 1$ steering vector of the ith source can be expressed as

$$\mathbf{a}(\theta_i,\phi_i)=\left[\exp\left(j\frac{2\pi}{\lambda}(x_1\sin\phi_i\sin\theta_i+y_1\sin\phi_i\cos\theta_i)\right),\ldots,\right.$$
$$\left.\times\exp\left(j\frac{2\pi}{\lambda}(x_M\sin\phi_i\sin\theta_i+y_M\sin\phi_i\cos\theta_i)\right)\right], \quad (7)$$

where θ_i and ϕ_i are the ith source DOAs (ϕ_i is the angle of the ith source DOA vector with respect to the z-axis and θ_i is the angle between the projection of the ith source DOA vector on the xy-plane and the y-axis). In this case, the likelihood ratio should be maximized for all values of θ and ϕ. In other words

$$\mathcal{L}_\ell(\mathbf{x})=\max_{\theta,\phi}\sum_{n=1}^{N}\frac{|\mathbf{a}^H(\theta,\phi)\mathbf{P}_{\ell-1}^{\perp}\mathbf{x}(n)|^2}{\mathbf{a}^H(\theta,\phi)\mathbf{P}_{\ell-1}^{\perp}\mathbf{a}(\theta,\phi)}. \quad (8)$$

4. Reducing the computational complexity of the proposed method and computational complexity analysis

In this section, first we develop a recursive form for $\mathbf{P}_{\ell-1}^{\perp}$ given by (6) and then we employ Fourier series expansion and discrete Fourier transform (DFT) to reduce the computational complexity of (5). After reducing the computational complexity, we will analyze the computational complexity of the proposed method.

4.1. Recursive form of $\mathbf{P}_{\ell}^{\perp}$

According to [17], $\mathbf{P}_{\ell}^{\perp}$ can be written as follows

$$\mathbf{P}_{\ell}^{\perp}=\mathbf{P}_{\ell-1}^{\perp}-\boldsymbol{\nu}_\ell\boldsymbol{\nu}_\ell^H, \quad (9)$$

where

$$\boldsymbol{\nu}_\ell\triangleq\frac{\mathbf{P}_{\ell-1}^{\perp}\mathbf{a}_\ell}{\|\mathbf{P}_{\ell-1}^{\perp}\mathbf{a}_\ell\|}. \quad (10)$$

4.2. Approximate form of $\mathcal{L}_\ell(\mathbf{x})$

If we define $f(\theta)\triangleq\sum_{n=1}^{N}\left|\mathbf{a}^H(\theta)\mathbf{P}_{\ell}^{\perp}\mathbf{x}(n)\right|^2$, in order to calculate $f(\theta)$ at K_1 points, the order of computation is going to be $\mathcal{O}(K_1M^2NL)$ operations for L number of sources. Similar to the method proposed in [8], we can approximate $f(\theta)$ to reduce the computational complexity.

Since $f(\theta)$ is periodic in θ with period 2π, it can be expressed by its Fourier series expansion. The Fourier coefficients are given by

$$F_k=\frac{1}{2\pi}\int_{-\pi}^{\pi}f(\theta)e^{-jk\theta}d\theta. \quad (11)$$

Table 1
The orders of the computational complexities of the proposed method, spectral music.

Algorithm	Computational complexity
Spectral MUSIC	$\mathcal{O}(M^3+K_1(M-L)M+M^2N)$
Proposed method	$\mathcal{O}([KM^2N+K\log_2K+K_1\log_2K_1+M^2]L)$

Truncating the Fourier series to $2K-1$ points, the function $f(\theta)$ can be approximated as

$$f(\theta)\simeq\sum_{k=-(K-1)}^{(K-1)}F_ke^{jk\theta}. \quad (12)$$

Using a numerical approximation of (11) we will have

$$F_k\simeq\frac{1}{2\pi}\sum_{r=-(K-1)}^{K-1}f(r\Delta\theta)e^{-jkr\Delta\theta}\Delta\theta\triangleq\hat{F}_k, \quad (13)$$

Where $\Delta\theta=2\pi/(2K-1)$. Now, we can compute (13) using the DFT. Using the above approximation, (12) can be rewritten as

$$f(\theta)\simeq\sum_{k=-(K-1)}^{K-1}\hat{F}_ke^{jk\theta}\triangleq\tilde{f}(\theta). \quad (14)$$

Now, let us use zero-padding in (14) to increase the number of values from $2K-1$ to $2K_1-1$ where $2K_1-1$ is the required number of search steps over θ ($K_1\gg K$). Then (14) becomes

$$\tilde{f}(\theta)=\sum_{k=-(K_1-1)}^{K_1-1}\tilde{F}_ke^{jk\theta}, \quad (15)$$

where

$$\tilde{F}_k=\begin{cases}\hat{F}_k, & \text{if } |k|\le K-1\\ 0, & \text{if } K-1<|k|\le K_1-1.\end{cases} \quad (16)$$

In short, at first, $f(\theta)$ must be directly calculated at the $2K-1$ point. Then using these values and (13), $\hat{F}_k$ must be calculated at the $2K-1$ point. At last using the zero-padding and (15), $\tilde{f}(\theta)$ must be calculated at the $2K_1-1$ point using IDFT. Note that if we don't use this section, $f(\theta)$ must be directly calculated at the $2K_1-1$ point.

4.3. Computational complexity analysis

The order of the computational complexities of the proposed method and spectral MUSIC have been compared in Table 1. Note that the computational complexity of the eigen-decomposition step is represented by the term $\mathcal{O}(M^3)$. The computation of K_1 samples of the MUSIC null-spectrum function requires $\mathcal{O}(K_1(M-L)M)$ operations and computing the sample covariance matrix needs $\mathcal{O}(M^2N)$ operations. To obtain the order of the computational complexity of the proposed method, first we calculate $f(\theta)$ in $2K-1$ points. The order of this calculation is $\mathcal{O}(KM^2N)$. The order of computation of $2K-1$ samples of $\hat{F}_k$ is $\mathcal{O}(K\log_2K)$. One can show that the complexity order of $f(\theta)$ in (15) is $\mathcal{O}(K_1\log_2K_1)$ operations. Finally, the complexity of $\mathbf{P}_{\ell}^{\perp}$ in Eq. (9) can be computed to be $\mathcal{O}(M^2)$. It should be noted that these computations must be repeated L times and also note that $K_1\gg K$. These results are summarized in Table 1.

As can be seen from Table 1, the computational complexities of the methods depend on the scenario and array parameters. The value of K_1 must be chosen to make sure that the errors caused by the angular grid step size are negligible relative to the value of the RMSE. Consider a numerical scenario where the number of elements is $M=12$, the number of snapshots is $N=10$,

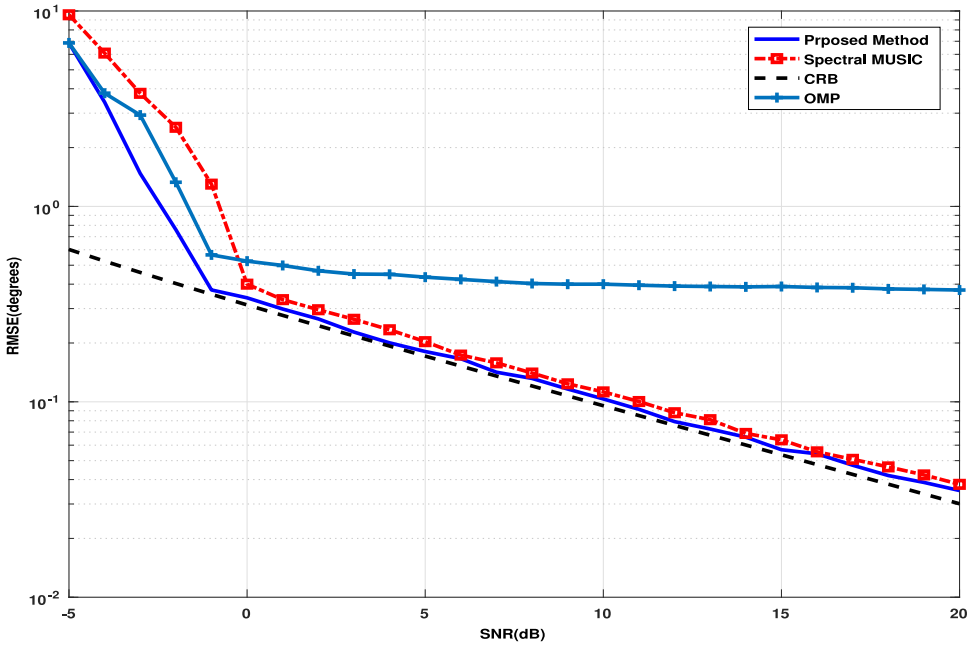

Fig. 1. DOA estimation RMSEs versus SNR for two uncorrelated sources at $\theta_1 = -5^\circ$ and $\theta_2 = 10^\circ$ ($N = 10$). The NUA of Table 2 with $M = 12$ is considered.

the number of sources $L = 2$, $K = 64$ and $K_1 = 8192$. In this scenario the dominant term of the computational complexity for the spectral MUSIC is $K_1(M-L)M$ which is equal to 983, 040. For the proposed method the terms KM^2NL and $K_1 \log_2 K_1 L$ are dominant that are equal to 184, 320 and 212, 992 respectively. Therefore, in this scenario spectral MUSIC needs more computations than the proposed method. Please note that the spectral MUSIC algorithm must be accompanied by an enumeration algorithm. Consequently, the computational complexity of this enumeration algorithm must be added to that of spectral MUSIC method but the proposed method estimates the number and the DOA of the sources jointly.

Please note that, without the method provided in previous subsection, calculation of $f(\theta)$ at K_1 points needs $\mathcal{O}(K_1M^2NL)$ operations for L number of sources that is equal to 23,592,960. This shows that the method presented in Section 4.2 reduces the computational complexity dramatically.

Remark 2. For the two-dimensional case, the computational complexity of the proposed method increases proportional to the search step size of ϕ.

5. Performance analysis

One of the most important metrics in the performance analysis of a source enumeration algorithm is the probability of correct detection of the number of sources. In this section, we derive a performance bound on the probability of correct detection by assuming that the directions of the sources are known. Given the number of sources is equal to L, the conditional correct detection probability can be stated as:

$$P_c|_{\ell=L} = \Pr(\mathcal{L}_1(\mathbf{x}) > \eta_1, \mathcal{L}_2(\mathbf{x}) > \eta_2, \ldots, \mathcal{L}_L(\mathbf{x}) > \eta_L, \mathcal{L}_{L+1}(\mathbf{x}) < \eta_{L+1}), \tag{17}$$

where $\eta_1, \eta_2, \ldots, \eta_{L+1}$ are the detection thresholds. Now consider the following lemma:

Lemma 1. *$\mathcal{L}_i(\mathbf{x})$ and $\mathcal{L}_j(\mathbf{x})$ are independent for $i \neq j$.*

Proof. See Appendix B. □

Using Lemma 1, the Eq. (17) can be stated as

$$P_c|_{\ell=L} = \Pr(\mathcal{L}_1(\mathbf{x}) > \eta_1)\Pr(\mathcal{L}_2(\mathbf{x}) > \eta_2)\ldots\Pr(\mathcal{L}_L(\mathbf{x}) > \eta_L) \times \Pr(\mathcal{L}_{L+1}(\mathbf{x}) < \eta_{L+1}). \tag{18}$$

Defining the random variable $z(n)$ as

$$z(n) \triangleq \frac{\mathbf{a}_i^H \mathbf{P}_{i-1}^{\perp} \mathbf{x}(n)}{\sqrt{\mathbf{a}_i^H \mathbf{P}_{i-1}^{\perp} \mathbf{a}_i \sigma^2}}, \tag{19}$$

$\mathcal{L}_i(\mathbf{x})$ in (5) is equivalent to

$$\mathcal{L}_i(\mathbf{x}) \equiv \mathcal{L}_i(z) = \sum_{n=1}^{N} |z(n)|^2, \tag{20}$$

where $z(n)$; $n = 1, \ldots, N$ are N independent, normally distributed complex random variables with the mean $\mu_i(n)$ and the unit variance in which $\mu_i(n)$ is given by

$$\mu_i(n) = \frac{\mathbf{a}_i^H \mathbf{P}_{i-1}^{\perp} \mathbf{A}_L \mathbf{s}_L(n)}{\sqrt{\mathbf{a}_i^H \mathbf{P}_{i-1}^{\perp} \mathbf{a}_i \sigma^2}}. \tag{21}$$

Thus, $\mathcal{L}_i(z)$ is a random variable that has noncentral chi-squared distribution with $2N$ degrees of freedom and non-centrality parameter λ_i, which is related to $\mu_i(n)$ as

$$\lambda_i = \sum_{n=1}^{N} |\mu_i(n)|^2 = \sum_{n=1}^{N} \frac{\mathbf{a}_i^H \mathbf{P}_{i-1}^{\perp} \mathbf{A}_L \mathbf{s}_L(n) \mathbf{s}_L(n)^H \mathbf{A}_L^H \mathbf{P}_{i-1}^{\perp} \mathbf{a}_i}{\mathbf{a}_i^H \mathbf{P}_{i-1}^{\perp} \mathbf{a}_i \sigma^2}. \tag{22}$$

Using the cumulative distribution function of the non-central chi-squared distribution, we have [21]

$$\Pr(\mathcal{L}_i(\mathbf{x}) > \eta_i) = \mathcal{Q}_N\left(\sqrt{\lambda_i}, \sqrt{\eta_i}\right), \tag{23}$$

where $\mathcal{Q}_N(a, b)$ is the Marcum Q-function defined as [22]

$$\mathcal{Q}_N(a, b) = \int_b^{\infty} x \left(\frac{x}{a}\right)^{N-1} \exp\left(-\frac{x^2 + a^2}{2}\right) I_{N-1}(ax) \mathrm{d}x, \tag{24}$$

and I_{N-1} is the modified Bessel function of order $N - 1$.

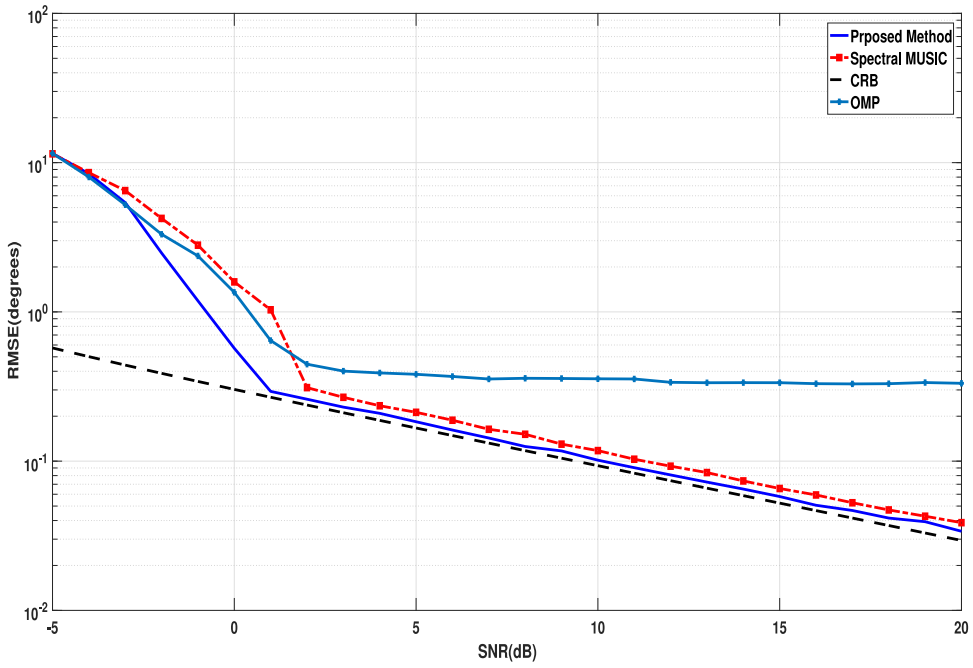

Fig. 2. DOA estimation RMSEs versus SNR for three uncorrelated sources at $\theta_1 = -5^\circ$, $\theta_2 = 10^\circ$ and $\theta_3 = 30^\circ$ ($N = 10$). The NUA of Table 2 with $M = 12$ is considered.

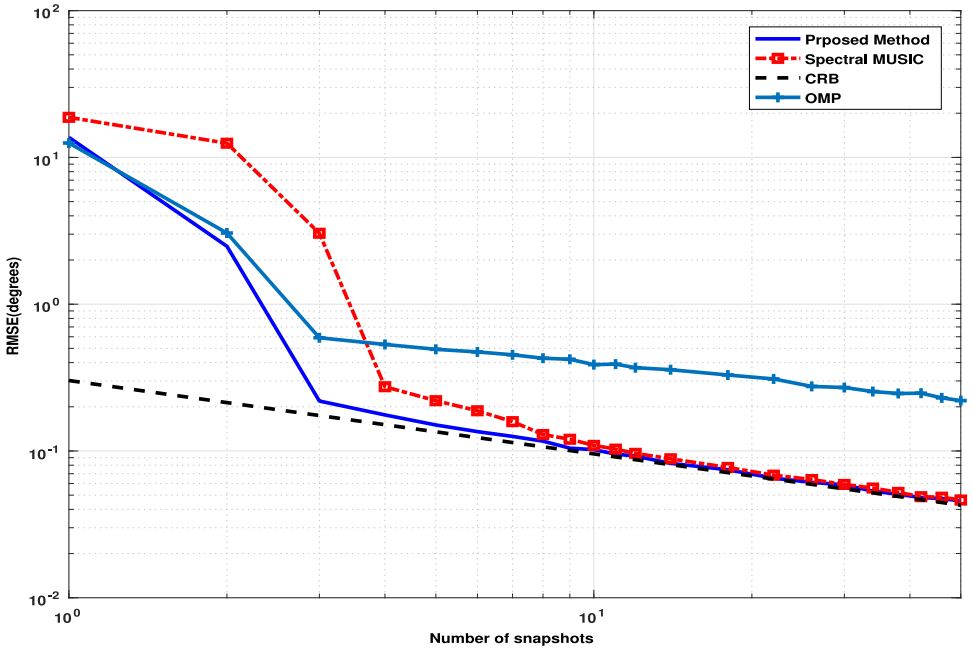

Fig. 3. DOA estimation RMSEs versus N for two uncorrelated sources at $\theta_1 = -5^\circ$ and $\theta_2 = 10^\circ$ (SNR=10 dB). The NUA of Table 2 with $M = 12$ is considered.

Thus, (18) can be stated as

$$P_c|_{\ell=L} = \mathcal{Q}_N\left(\sqrt{\lambda_1}, \sqrt{\eta_1}\right)\mathcal{Q}_N\left(\sqrt{\lambda_2}, \sqrt{\eta_2}\right)\ldots \mathcal{Q}_N\left(\sqrt{\lambda_L}, \sqrt{\eta_L}\right)\left(1 - \mathcal{Q}_N\left(\sqrt{\lambda_{L+1}}, \sqrt{\eta_{L+1}}\right)\right). \quad (25)$$

For the cases where there is only one or two sources we can simplify the correct detection probability as follows:

Case 1 One source ($L = 1$):
In this case, we have

$$P_c|_{\ell=1} = \Pr(\mathcal{L}_1(\mathbf{x}) > \eta_1)\Pr(\mathcal{L}_2(\mathbf{x}) < \eta_2). \quad (26)$$

Hence, we have

$$P_c|_{\ell=1} = \mathcal{Q}_N\left(\sqrt{\frac{M\sum_{n=1}^{N}|s_1(n)|^2}{\sigma^2}}, \sqrt{\eta_1}\right) F_{\chi^2_{2N}}(\eta_2). \quad (27)$$

where $F_{\chi^2_{2N}}(\eta_2)$ is the central chi-squared distribution function with $2N$ degrees of freedom [22].

Case 2 Two sources ($L = 2$):
In this case, we have

$$P_c|_{\ell=2} = \Pr(\mathcal{L}_1(\mathbf{x}) > \eta_1)\Pr(\mathcal{L}_2(\mathbf{x}) > \eta_2)\Pr(\mathcal{L}_3(\mathbf{x}) < \eta_3). \quad (28)$$

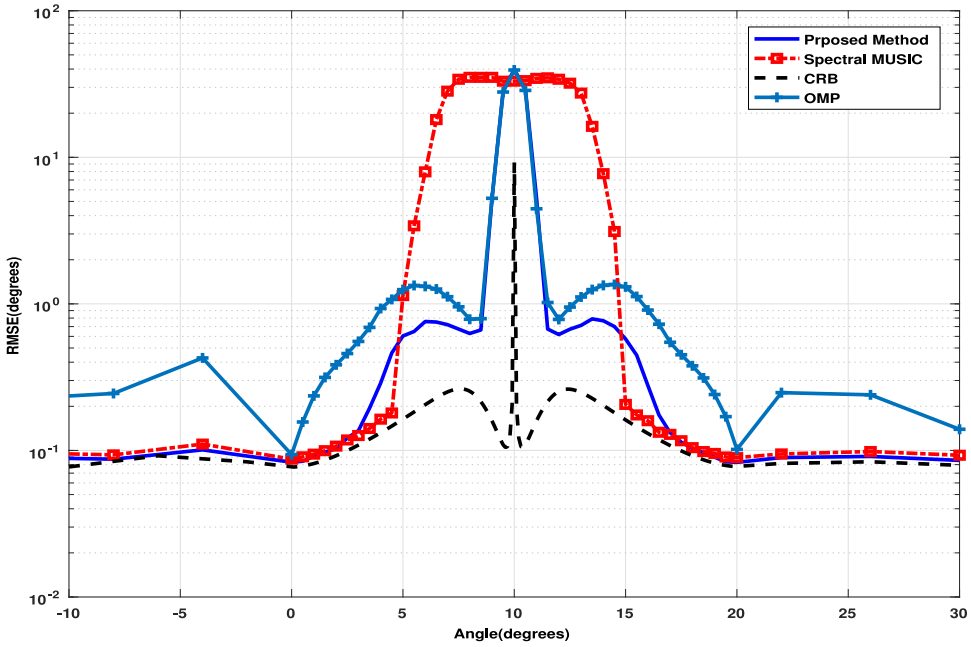

Fig. 4. DOA estimation RMSEs for two uncorrelated sources. One is fixed at 10° and the second has swept (SNR = 10 dB and $N = 10$). The NUA of Table 2 with $M = 12$ is considered.

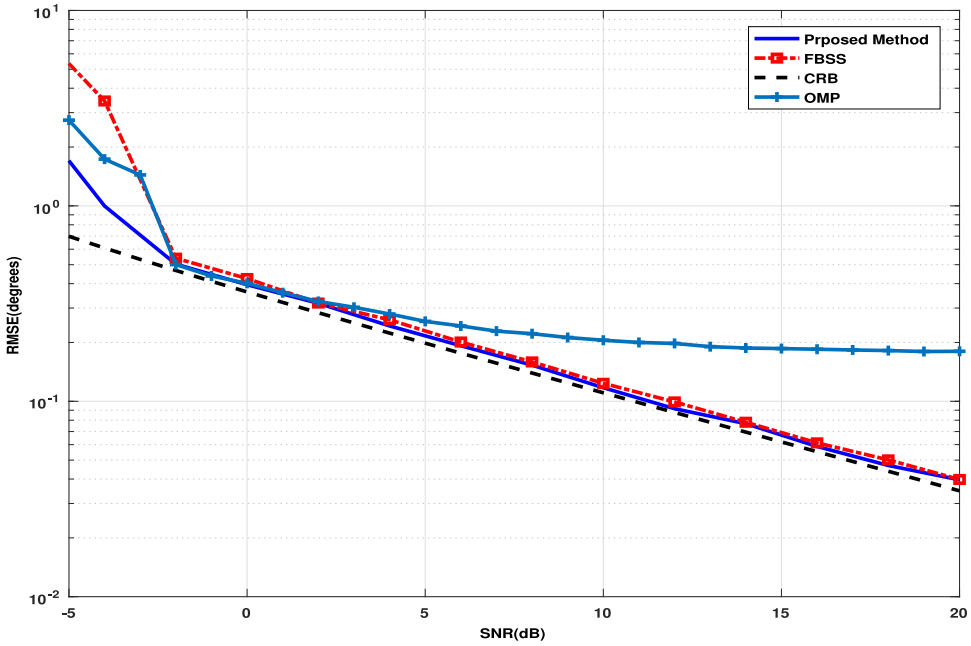

Fig. 5. DOA estimation RMSEs versus SNR for two fully correlated sources at $\theta_1 = -5^\circ$ and $\theta_2 = 10^\circ$ ($N = 10$). A ULA with $M = 12$ and a sensor spacing equal to $\frac{\lambda}{2}$ is considered.

Thus, we have

$$P_c|_{\ell=2} = \mathcal{Q}_N\left(\sqrt{\frac{M\sum_{n=1}^{N}|s_1(n)|^2}{\sigma^2}}, \sqrt{\eta_1}\right) \times \mathcal{Q}_N\left(\sqrt{\frac{\mathbf{a}_2^H\mathbf{P}_1^{\perp}\mathbf{a}_2\sum_{n=1}^{N}|s_2(n)|^2}{\sigma^2}}, \sqrt{\eta_2}\right) F_{\chi^2_{2N}}(\eta_3). \quad (29)$$

It is noteworthy that the values of the thresholds at each stage are dependent on the false alarm probability (P_{fa}) and the value of false alarm probability will affect the correct detection probability. In fact, in the proposed method, the correct detection probability is obtained from the product of the detection probability at each stage and $1 - P_{fa}$ of the final stage. Therefore, the probability of false alarm must be selected in such a manner that the probability of detection becomes sufficiently large at each stage while P_{fa} remains small enough.

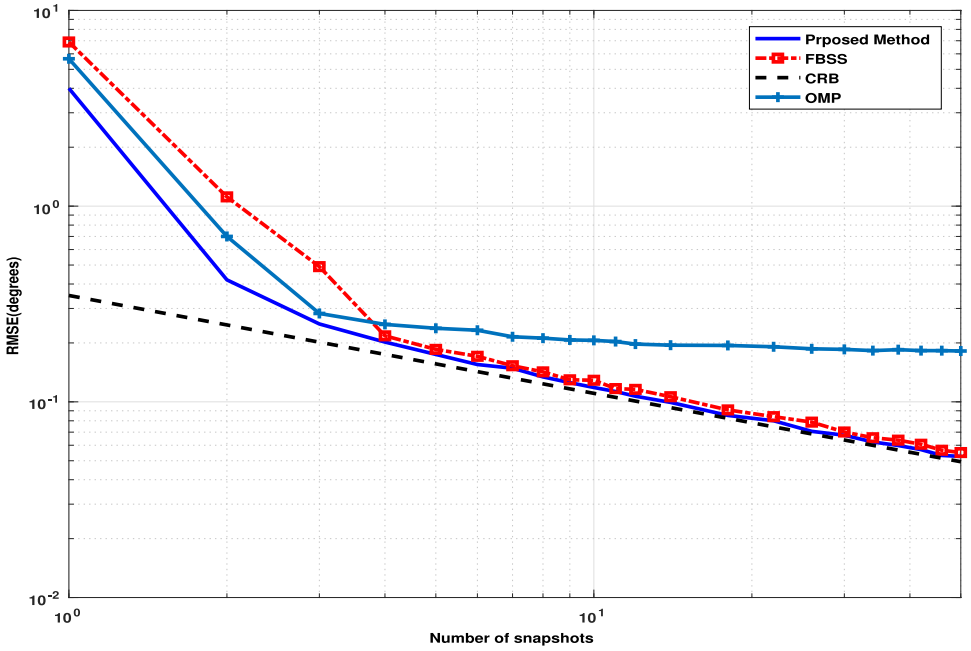

Fig. 6. DOA estimation RMSEs versus N for two fully correlated sources at $\theta_1 = -5^\circ$ and $\theta_2 = 10^\circ$ (SNR = 10 dB). A ULA with $M = 12$ and a sensor spacing equal to $\frac{\lambda}{2}$ is considered.

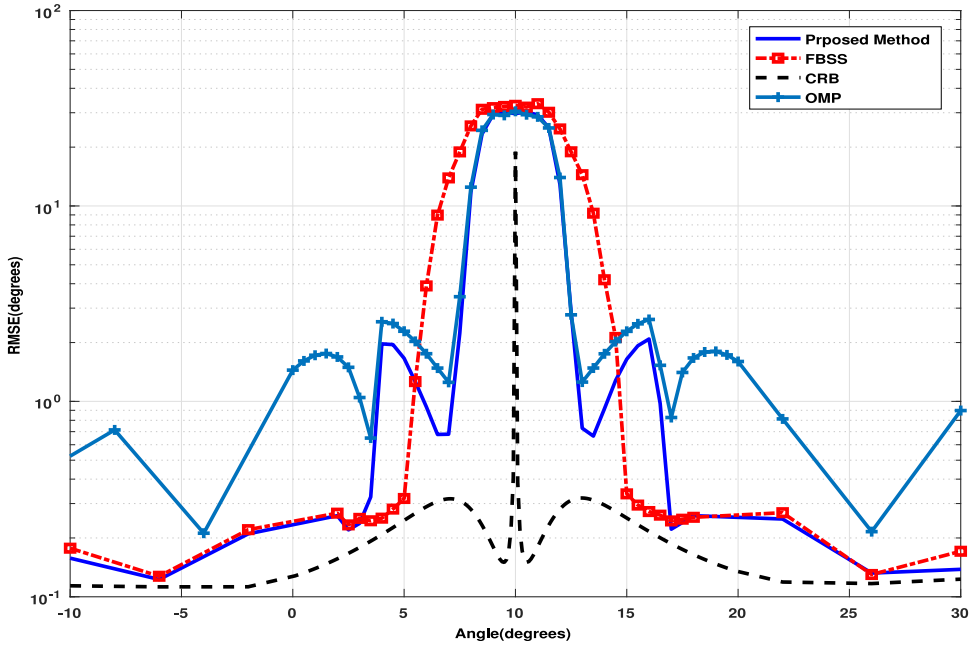

Fig. 7. DOA estimation RMSEs for two fully correlated sources. One is fixed at 10° and the second has swept (SNR = 10 dB and $N = 10$). A ULA with $M = 12$ and a sensor spacing equal to $\frac{\lambda}{2}$ is considered.

6. Simulation results

In this section, a number of numerical examples are presented. For DOA estimation performance analysis, the Root Mean Square Error (RMSE) is considered. For each of the performance comparisons, 1000 independent Monte Carlo trials have been used. In DOA estimation performance examples, the comparison is made among the proposed method, the spectral MUSIC and OMP for uncorrelated sources, and also FBSS and OMP for fully correlated sources. The benchmark is considered to be the Cramer Rao bound (CRB) [3]. In addition, for the source number detection examples, the proposed method is compared with the MDL method. The range of θ is $-90^\circ < \theta < 90^\circ$ and the likelihood ratio is computed in 8192 point.

Fig. 1 demonstrates the DOA estimation RMSEs of the proposed method, spectral MUSIC and OMP versus the sensor signal-to-noise ratio (SNR). The number of snapshots is set to be $N = 10$. Two equal power uncorrelated signal sources are assumed to impinge on the array from the directions $\theta_1 = -5^\circ$ and $\theta_2 = 10^\circ$. A nonuniform array (NUA) of 12 sensors is considered. This type of array geometry is designed in [23] for azimuthal DOA estimation. The locations of sensors of this array are given in Table 2. It can be seen from Fig. 1 that the proposed method outperforms the OMP and spectral MUSIC. OMP performance increases with a very small

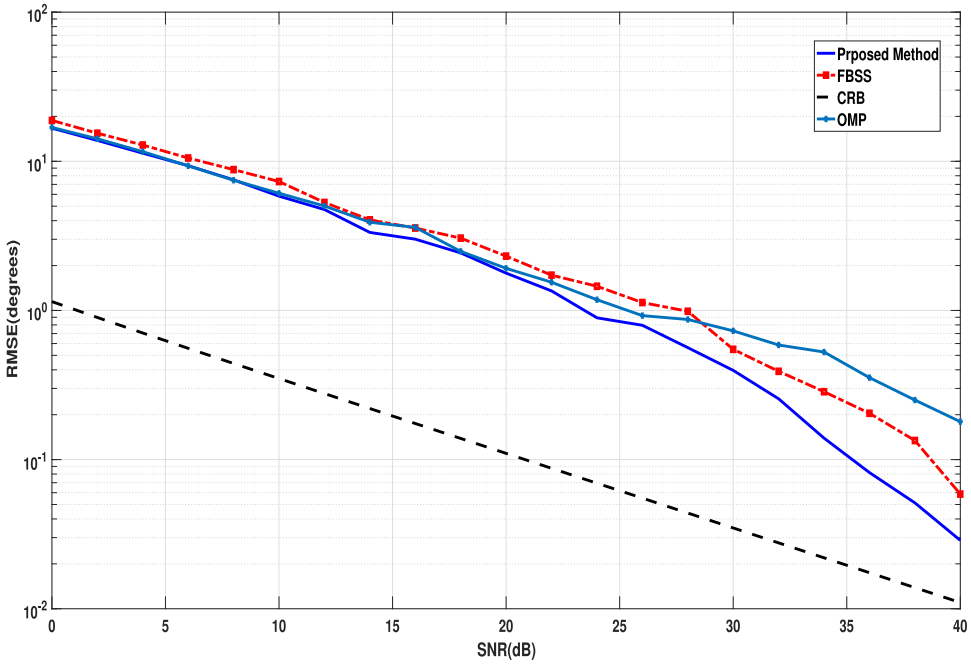

Fig. 8. DOA estimation RMSEs versus SNR in the case of single snapshot ($N = 1$) for two fully correlated sources at $\theta_1 = -5^\circ$ and $\theta_2 = 10^\circ$. A ULA with $M = 12$ and a sensor spacing equal to $\frac{\lambda}{2}$ is considered.

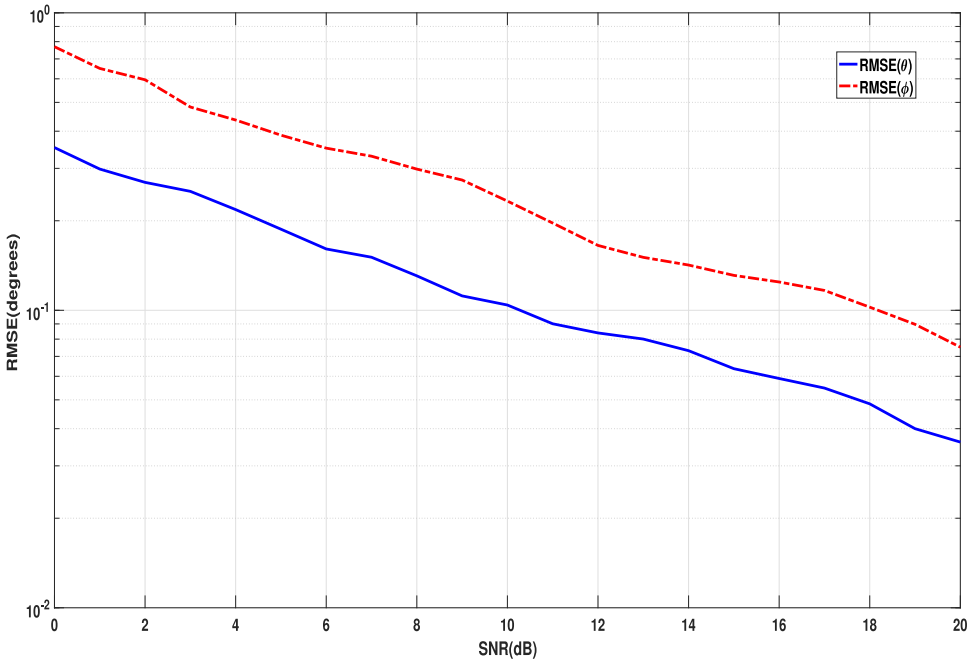

Fig. 9. Two-dimensional DOA estimation RMSEs versus SNR for the proposed method. Two uncorrelated sources at ($\theta_1 = -5^\circ$, $\phi_1 = 60^\circ$) and ($\theta_2 = 10^\circ$, $\phi_2 = 70^\circ$) are considered. The NUA of Table 2 with $M = 12$ is used and $N = 10$.

rate as the SNR increases. The reason is that the signal components cancellation is not done properly due to the DOA estimation error of the previous stage. Therefore, the signal residuals are not sufficiently small and affect DOA estimation performance of the next stage. The similar simulation with different number of sources is considered in Fig. 2. The number of sources is considered to be three in this simulation. The same performance behavior is observed as previous example.

Fig. 3 depicts the RSME for a given SNR (SNR = 10 dB) versus the number of snapshots for the source directions $\theta_1 = -5^\circ$ and $\theta_2 = 10^\circ$ and the same array configuration. The sources are considered to be uncorrelated in this example. It is observed that the performance of the proposed method is better in comparison with the spectral MUSIC and OMP method. As it can be seen, that the spectral MUSIC does not have a good performance when the number of snapshots is small. This is due to the fact that in this case an accurate estimation of the sample covariance matrix is not provided.

In Fig. 4 there are two uncorrelated sources, one is fixed at $\theta = 10^\circ$ and the other sweeps from -10° to 30°. The SNR is equal to 10 dB and the array geometry is the same as the first example. As can be seen, the proposed method has a better perfor-

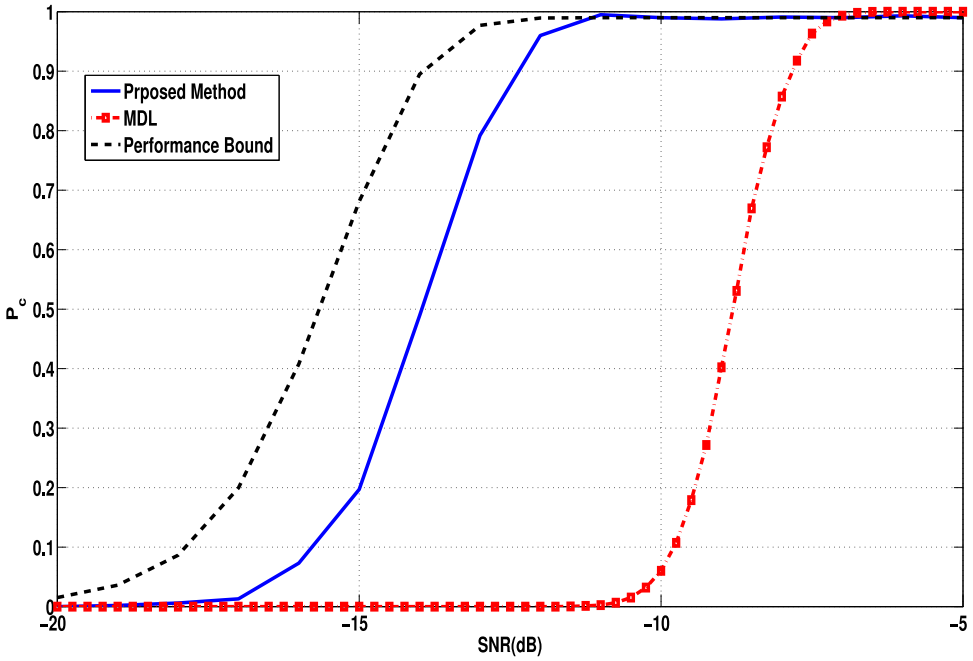

Fig. 10. Probability of correct detection of the number of sources versus SNR for two uncorrelated sources at $\theta_1 = -5^\circ$ and $\theta_2 = 10^\circ$ ($N = 100$). The NUA of Table 2 with $M = 12$ is considered.

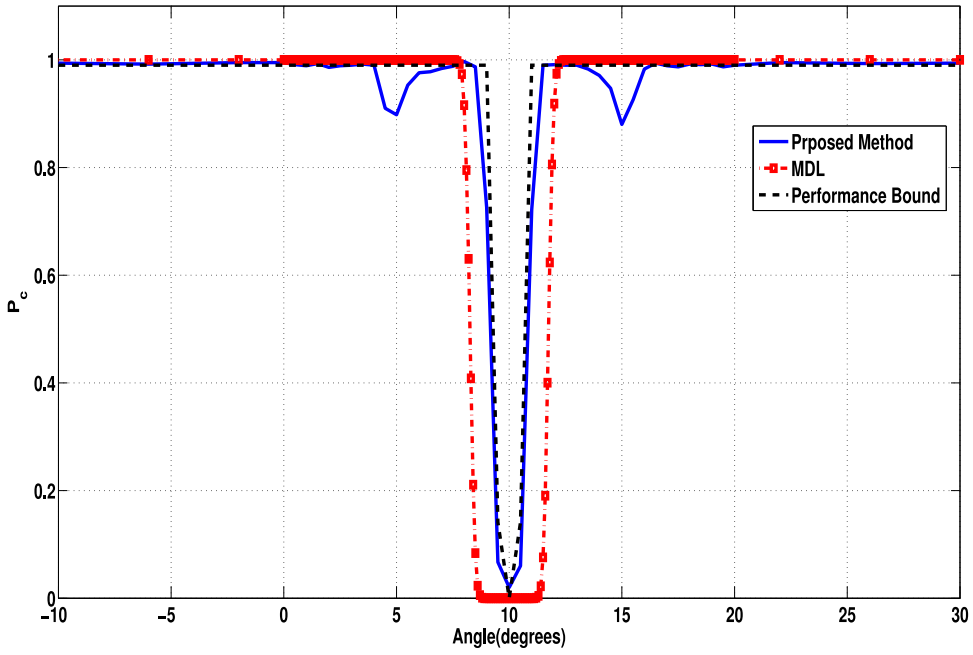

Fig. 11. Probability of correct detection of the number of sources for two uncorrelated sources. One source is fixed at 10° and the second has swept (SNR= 0 dB and $N = 100$). The NUA with $M = 12$ of Table 2 is considered.

mance in comparison with the spectral MUSIC and OMP for two closely located sources. It can be seen that the proposed method and the OMP, encounter a performance degradation in some source angles. The reason of this performance degradation is that these two methods can be seen as a type of spatial filtering technique. Therefore, this degradation in some source angles results from the side lobe effects. The location and amount of performance degradation depends on array geometry, SNR value and the DOA estimation method. Spectral MUSIC is based on the signal and noise subspaces. Consequently, the performance behavior of this method is different from the proposed method and OMP.

For fully correlated sources, the same scenarios as in the Figs. 1, 3 and 4 are considered in Figs. 5–7, respectively. Since the sources are fully correlated, the spectral MUSIC method fails. Therefore, in these simulations the comparison is carried out between the proposed method, the FBSS and OMP methods. It should be noted that the FBSS method is solely applicable to uniform arrays. Hence, we have considered a ULA with $M = 12$ and a sensor spacing equal to $\frac{\lambda}{2}$. It is seen that the proposed method usually outperforms the FBSS and OMP methods in the fully correlated source case. In Fig. 8 a single snapshot scenario is considered. The sources are

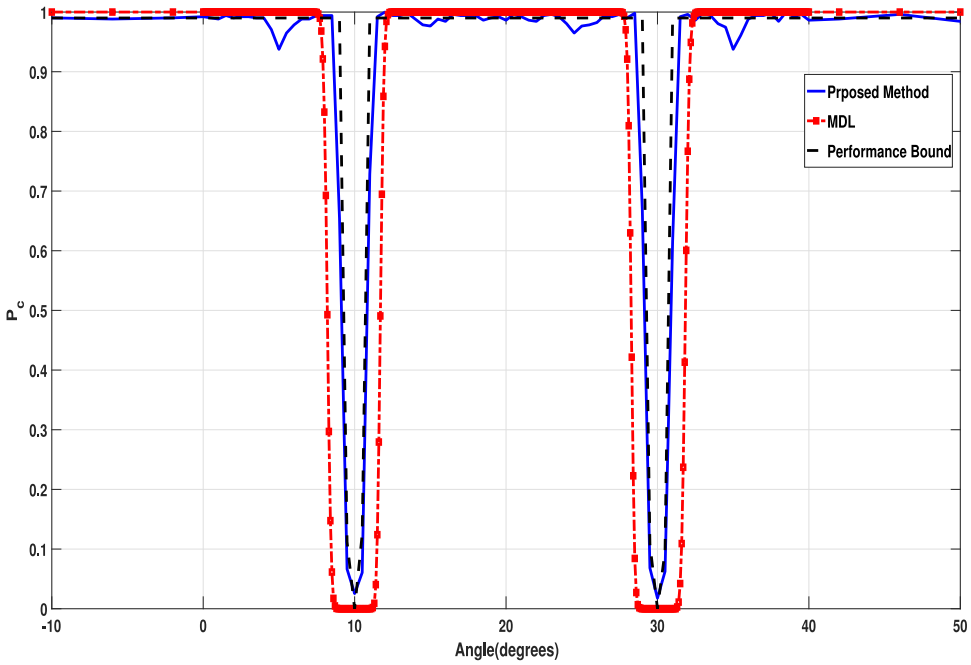

Fig. 12. Probability of correct detection of the number of sources for three uncorrelated sources. Two sources are fixed at 10° , 30° and the third has swept (SNR= 0 dB and $N = 100$). The NUA with $M = 12$ of Table 2 is considered.

Table 2
Sensor locations Of The NUA array.

M	x_m/λ	y_m/λ
1	−0.016	3.336
2	−1.776	−2.892
3	−1.825	3.313
4	3.811	0.300
5	−2.859	−0.170
6	3.849	−0.051
7	3.001	2.069
8	−2.372	2.114
9	2.204	−2.123
10	0.195	−3.250
11	−2.142	0.535
12	−2.069	−3.183

fully correlated. As it can be seen, the proposed method is also applicable to the single snapshot case.

We consider a two-dimensional scenario in Fig. 9. Two uncorrelated sources are assumed at the directions ($\theta_1 = -5^\circ$, $\phi_1 = 60^\circ$) and ($\theta_2 = 10^\circ$, $\phi_2 = 70^\circ$). This figure demonstrates the RMSEs in ϕ and θ directions versus SNR for the proposed method. As it can be seen, we can apply the proposed method to the two-dimensional scenarios. Fig. 10 shows the probability of correct detection of the number of sources versus SNR. The false alarm probability is set to 0.01 in each stage. As a result, the maximum value of correct detection probability tends to be 0.99, which is a suitable value for correct detection probability. The threshold values are obtained by the Monte Carlo simulations to achieve the mentioned false alarm probability. Note that the noise variance is assumed to be known a priori. It is observed that there is a dramatic performance difference between the proposed method and the MDL method. It can also be observed that the performance gap between the proposed method and the analytical performance bound derived in Eq. (29), is about 2 dB. It should be noted that the probability of correct detection of the proposed method is obtained using Monte Carlo simulation. In Fig. 11, one source is fixed at $\theta = 10^\circ$ and the other sweeps from -10° to 30° with SNR = 0 dB. It can be seen that the proposed method can provide a better source number detection when the sources are close to each other. In Fig. 12, the number of sources is three. The directions of two sources are fixed at $\theta_1 = 10^\circ$, $\theta_2 = 30^\circ$ and the third source sweeps from -10° to 50° with SNR = 0 dB. It can be seen that the proposed method has a good performance in the case of three sources.

7. Conclusion

In this paper we proposed a sequential algorithm to solve the problem of the joint direction-of-arrival (DOA) estimation and source number detection for arrays with arbitrary geometry. This algorithm results from solving a sequential hypothesis testing problem. Simulation results show that the proposed algorithm usually has a performance better than the spectral MUSIC and FBSS method in the case of low SNR or small number of snapshots. In addition, the performance of the proposed method in source number detection is usually better than the MDL method.

Appendix A. Derivation of relation (5)

In order to solve the hypothesis testing problem (3), we apply a suitable transformation to the received signal. Using this transformation, the unknown parameters will be reduced to only two parameters that are $s_\ell(n)$ and the azimuth direction of the ℓth source. To do this, we use the singular value decomposition (SVD) to rewrite $\mathbf{A}_{\ell-1}$ as

$$\mathbf{A}_{\ell-1} = \begin{bmatrix}\mathbf{U}_1 & \mathbf{U}_2\end{bmatrix}\begin{bmatrix}\sum_{\ell-1} & \mathbf{0} \\ \mathbf{0} & \mathbf{0}\end{bmatrix}\begin{bmatrix}\mathbf{V}_1^H \\ \mathbf{V}_2^H\end{bmatrix}, \tag{A.1}$$

where $\mathbf{U}_1$ and $\mathbf{U}_2$ are $M \times (\ell - 1)$ and $M \times (M - \ell + 1)$ orthogonal matrices which span the columns of the $\mathbf{A}_{\ell-1}$ and orthogonal space to columns of the $\mathbf{A}_{\ell-1}$, respectively. In other words, we have

$$\mathbf{U}_2^H \mathbf{A}_{\ell-1} = \mathbf{0}. \tag{A.2}$$

Multiplying the received signal from left side by $\mathbf{U}_2^H$, (3) can be rewritten as

$$\begin{cases} \mathcal{H}_0^{(\ell)} : \mathbf{x_u}(n) = \mathbf{w_u}(n), & n = 1, \ldots, N \\ \mathcal{H}_1^{(\ell)} : \mathbf{x_u}(n) = \mathbf{a}_\ell^{\mathbf{u}} s_\ell(n) + \mathbf{w_u}(n), & n = 1, \ldots, N, \end{cases} \tag{A.3}$$

where $\mathbf{x}_u(n) \triangleq \mathbf{U}_2^H \mathbf{x}(n)$, $\mathbf{a}_\ell^u \triangleq \mathbf{U}_2^H \mathbf{a}_\ell$ and $\mathbf{w_u}(n) \triangleq \mathbf{U}_2^H \mathbf{w}(n)$. Since $\mathbf{U}_2^H \mathbf{U}_2 = \mathbf{I}$ and $\mathbf{w}(n)$ is an $M \times 1$ vector of the Gaussian noise with zero mean and the covariance matrix $\sigma^2\mathbf{I}$, $\mathbf{w_u}(n)$ is also an $(M-\ell+1)\times 1$ vector of the Gaussian noise with zero mean and the covariance matrix $\sigma^2\mathbf{I}$.

To obtain the GLR detector for this composite hypothesis testing problem, the Maximum Likelihood (ML) estimate of the unknown paremeters should be inserted into the probability density function (PDF) under hypotheses $\mathcal{H}_0^{(\ell)}$ and $\mathcal{H}_1^{(\ell)}$. According to the (A.3), the PDF under each assumption can be written as

$$f(\mathbf{x}_u; \mathcal{H}_0^{(\ell)}) = \left(\frac{1}{\pi\sigma^2}\right)^{(N(M-\ell+1))} \exp\left(-\frac{\sum_{n=1}^N \|\mathbf{x}_u(n)\|^2}{\sigma^2}\right), \tag{A.4}$$

$$f(\mathbf{x}_u; \mathcal{H}_1^{(\ell)}) = \left(\frac{1}{\pi\sigma^2}\right)^{(N(M-\ell+1))} \exp\left(-\frac{\sum_{n=1}^N \|\mathbf{x}_u(n) - \mathbf{a}_\ell^u s_\ell(n)\|^2}{\sigma^2}\right). \tag{A.5}$$

It is not difficult to show that the ML estimates of the unknown parameters $s_\ell(n)$ and the azimuth direction of the ℓth source under the $\mathcal{H}_1^{(\ell)}$ hypothesis are

$$\mathcal{H}_1^{(\ell)} : \begin{cases} \hat{s}_\ell(n) = \frac{\mathbf{a}_\ell^{u^H} \mathbf{x}_u(n)}{\|\mathbf{a}_\ell^u\|^2} \\ \hat{\theta}_\ell = \arg\max_\theta (f(\mathbf{x}_u; \mathcal{H}_1^{(\ell)}, \hat{s}_\ell(n))). \end{cases} \tag{A.6}$$

Substituting (A.6) into (A.5), the likelihood ratio can be stated as

$$\mathcal{L}_\ell(\mathbf{x}_u) = \max_\theta \sum_{n=1}^N \frac{|\mathbf{a}^{uH}(\theta)\mathbf{x}_u(n)|^2}{\|\mathbf{a}^u(\theta)\|^2}. \tag{A.7}$$

Now we can write

$$\mathcal{L}_\ell(\mathbf{x}) = \max_\theta \sum_{n=1}^N \frac{|\mathbf{a}^H(\theta)\mathbf{U}_2\mathbf{U}_2^H\mathbf{x}(n)|^2}{\|\mathbf{a}^H(\theta)\mathbf{U}_2\|^2}. \tag{A.8}$$

From [24] we have

$$\mathbf{U}_2\mathbf{U}_2^H = \mathbf{I} - \mathbf{A}_{\ell-1}\left(\mathbf{A}_{\ell-1}^H\mathbf{A}_{\ell-1}\right)^{-1}\mathbf{A}_{\ell-1}^H \triangleq \mathbf{P}_{\ell-1}^\perp. \tag{A.9}$$

The final result can be achieved by substituting (A.9) into (A.8) as

$$\mathcal{L}_\ell(\mathbf{x}) = \max_\theta \sum_{n=1}^N \frac{|\mathbf{a}^H(\theta)\mathbf{P}_{\ell-1}^\perp\mathbf{x}(n)|^2}{\mathbf{a}^H(\theta)\mathbf{P}_{\ell-1}^\perp\mathbf{a}(\theta)} = \sum_{n=1}^N \frac{|\mathbf{a}_\ell{}^H\mathbf{P}_{\ell-1}^\perp\mathbf{x}(n)|^2}{\mathbf{a}_\ell{}^H\mathbf{P}_{\ell-1}^\perp\mathbf{a}_\ell} \underset{\mathcal{H}_0^{(\ell)}}{\overset{\mathcal{H}_1^{(\ell)}}{\gtrless}} \eta_\ell, \tag{A.10}$$

where $\mathbf{a}_\ell$ is the steering vector corresponding to the estimated direction for the ℓth source.

Appendix B. Proof of Lemma 1

In order to show that $\mathcal{L}_i(\mathbf{x})$ and $\mathcal{L}_j(\mathbf{x})$ $(i \neq j)$ are independent of each other, we use the following theorem.

Theorem 1. *Let* $\mathbf{z}$ *be an* $M \times 1$ *complex vector with the probability density function* $\mathcal{CN}(\boldsymbol{\mu}, \mathbf{C})$, *and let* $\mathbf{B}$ *and* $\mathbf{D}$ *be the* $M \times M$ *Hermitian matrices. If* $\mathbf{BCD} = \mathbf{0}$, *then the second-order statistics* $\mathbf{z}^H\mathbf{Bz}$ *and* $\mathbf{z}^H\mathbf{Dz}$ *are independent of each other [25].*

To use this theorem, we can rewrite $\mathcal{L}_i(\mathbf{x})$ and $\mathcal{L}_j(\mathbf{x})$ as an equivalent form

$$\begin{cases} \mathcal{L}_i(\mathbf{x}) \equiv \sum_{n=1}^N \mathbf{x}^H(n)\mathbf{P}_{i-1}^\perp\mathbf{a}_i\mathbf{a}_i^H\mathbf{P}_{i-1}^\perp\mathbf{x}(n) \\ \mathcal{L}_j(\mathbf{x}) \equiv \sum_{n=1}^N \mathbf{x}^H(n)\mathbf{P}_{j-1}^\perp\mathbf{a}_j\mathbf{a}_j^H\mathbf{P}_{j-1}^\perp\mathbf{x}(n). \end{cases} \tag{B.1}$$

Defining $\mathbf{B} \triangleq \mathbf{P}_{i-1}^\perp\mathbf{a}_i\mathbf{a}_i^H\mathbf{P}_{i-1}^\perp$, $\mathbf{D} \triangleq \mathbf{P}_{j-1}^\perp\mathbf{a}_j\mathbf{a}_j^H\mathbf{P}_{j-1}^\perp$ and $\mathbf{C} = \mathbf{I}$, if $\mathbf{BD} = \mathbf{0}$ then $\mathcal{L}_i(\mathbf{x})$ and $\mathcal{L}_j(\mathbf{x})$ $(i \neq j)$ are independent of each other according to the Theorem 1. Assuming $i < j$, we have

$$\mathbf{BD} = \mathbf{P}_{i-1}^\perp\mathbf{a}_i\mathbf{a}_i^H\mathbf{P}_{i-1}^\perp\mathbf{P}_{j-1}^\perp\mathbf{a}_j\mathbf{a}_j^H\mathbf{P}_{j-1}^\perp. \tag{B.2}$$

Now we have

$$\begin{cases} \mathbf{P}_{i-1}^\perp = \mathbf{I} - \mathbf{A}_{i-1}\left(\mathbf{A}_{i-1}^H\mathbf{A}_{i-1}\right)^{-1}\mathbf{A}_{i-1}^H \\ \mathbf{P}_{j-1}^\perp = \mathbf{I} - \mathbf{A}_{j-1}\left(\mathbf{A}_{j-1}^H\mathbf{A}_{j-1}\right)^{-1}\mathbf{A}_{j-1}^H, \end{cases} \tag{B.3}$$

where $\mathbf{A}_{i-1} = [\mathbf{a}_1, \ldots, \mathbf{a}_{i-1}]$ and $\mathbf{A}_{j-1} = [\mathbf{A}_{i-1}, \mathbf{a}_i \ldots, \mathbf{a}_{j-1}]$. Consequently

$$\begin{aligned} \mathbf{P}_{i-1}^\perp\mathbf{P}_{j-1}^\perp &= (\mathbf{I} - \mathbf{A}_{i-1}\left(\mathbf{A}_{i-1}^H\mathbf{A}_{i-1}\right)^{-1}\mathbf{A}_{i-1}^H)\mathbf{P}_{j-1}^\perp \\ &= \mathbf{P}_{j-1}^\perp - \mathbf{A}_{i-1}\left(\mathbf{A}_{i-1}^H\mathbf{A}_{i-1}\right)^{-1}\mathbf{A}_{i-1}^H\mathbf{P}_{j-1}^\perp. \end{aligned} \tag{B.4}$$

We know that $\mathbf{A}_{j-1}^H\mathbf{P}_{j-1}^\perp = \mathbf{0}$ and as a result $\mathbf{A}_{i-1}^H\mathbf{P}_{j-1}^\perp = \mathbf{0}$. Thus, we have

$$\mathbf{P}_{i-1}^\perp\mathbf{P}_{j-1}^\perp = \mathbf{P}_{j-1}^\perp. \tag{B.5}$$

Substituting (B.5) into (B.2) yields

$$\mathbf{BD} = \mathbf{P}_{i-1}^\perp\mathbf{a}_i\mathbf{a}_i^H\mathbf{P}_{j-1}^\perp\mathbf{a}_j\mathbf{a}_j^H\mathbf{P}_{j-1}^\perp. \tag{B.6}$$

It is clear that $\mathbf{a}_i^H\mathbf{P}_{j-1}^\perp = 0$. Therefore, $\mathbf{BD} = \mathbf{0}$ and the proof is complete.

References

[1] H.L. Van Trees, Optimum Array Processing, Part IV of Detection, Estimation and Modulation Theory, Wiley, New York, 2002. Chapter 1.
[2] A.M. Zoubir, M. Viberg, R. Chellappa, S. Theodoridis, Array and Statistical Signal Processing, vol. 3, Academic Press Library in Signal Processing, 2014. Chapter 20.
[3] E. Tuncer, B. Friedlander, Classical and Modern Direction-of-Arrival Estimation, Elsevier Inc., 2009. Chapters 1,4.
[4] M. Elbir, E. Tuncer, 2-d DOA and mutual coupling coefficient estimation for arbitrary array structures with single and multiple snapshots, Digital Signal Process. 54 (2016) 75–86.
[5] R.O. Schmidt, Multiple emitter location and signal parameter estimation, IEEE Trans. Antennas Propag. 34 (3) (1986) 276–280.
[6] A. Barabell, Improving the resolution performance of eigenstructure-based direction-finding algorithms, in: Proc. ICASSP, 1983, pp. 336–339.
[7] C.E. Kassis, J. Picheral, C. Mokbel, Advantages of nonuniform arrays using root–MUSIC, Signal Process. J. 90 (2) (2010) 689–695.
[8] M. Rubsamen, A.B. Gershman, Direction-of-arrival estimation for nonuniform sensor arrays: from manifold separation to fourier domain MUSIC methods, IEEE Trans. Signal Process. 57 (2) (2009) 588–599.
[9] A. Paulraj, R. Roy, T. Kailath, A subspace rotation approach to signal parameter estimation, Proc. IEEE 74 (7) (1986) 1044–1046.
[10] B. Friedlander, The root-MUSIC algorithm for direction finding with interpolated arrays, Signal Process. 30 (1993) 15–25.
[11] P. Hyberg, M. Jansson, B. Ottersten, Array interpolation and bias reduction, IEEE Trans. Signal Process. 52 (10) (2004) 2711–2720.
[12] P. Hyberg, M. Jansson, B. Ottersten, Array interpolation and DOA MSE reduction, IEEE Trans. Signal Process. 53 (12) (2005) 4464–4471.
[13] F. Belloni, A. Richter, V. Koivunen, DOA estimation via manifold separation for arbitrary array structures, IEEE Trans. Signal Process. 55 (10) (2007) 4800–4810.
[14] J.A. Hogbom, Aperture synthesis with non-regular distribution of interferometer baselines, Astron. Astrophys. Suppl. 15 (1974) 417–426.
[15] P. Stoica, R. Moses, Spectral Analysis of Signals, Prentice-Hall, 2005. Chapter 6.
[16] S.F. Cotter, B.D. Rao, K. Engan, K. Kreutz-Delgado, Sparse solutions to linear inverse problems with multiple measurement vectors, IEEE Trans. Signal Process. 53 (7) (2005) 2477–2488.
[17] S. Kay, Fundamentals of Statistical Signal Processing, Volume I: Estimation Theory, 1993. Chapter 8.
[18] S.U. Pillai, B.H. Kwon, Forward/backward spatial smoothing techniques for coherent signal identification, IEEE Trans. Signal Process. 37 (1) (1989) 8–15.
[19] M. Wax, I. Ziskind, Detection of the number of coherent signals by the MDL principle, IEEE Trans. Acoustics Speech Signal Process. 37 (8) (1989) 1190–1196.
[20] M. Wax, T. Kailath, Detection of signals by information theoretic criteria, IEEE Trans. Acoust. Speech Signal Process. 33 (2) (1985) 387–392.
[21] V.M. Kapinas, S.K. Mihos, G.K. Karagiannidis, On the monotonicity of the generalized marcum and nuttall q-functions, IEEE Trans. Inf. Theory 55 (8) (2009) 3701–3710.

[22] N.L. Johnson, S. Kotz, N. Balakrishnan, Continuous Univariate Distributions, vol. 2, Wiley, 1970.
[23] M. Rubsamen, A.B. Gershman, Sparse array design for azimuthal direction-of-arrival estimation, IEEE Trans. Signal Process 59 (12) (2011) 5957–5969.
[24] A.J. Laub, Matrix Analysis for Scientists and Engineers, Society for Industrial Mathematics, 2004. Chapter 7.
[25] C. Alvin, G. Rencher, S. Bruce, Linear Models in Statistics, Wiley, 2008. Chapter 4.